arXiv:0711.1395v4 [hep-th] 9 Feb 2008

WU-AP/277/07

Bulk scalar emission from a rotating black hole pierced by a tense brane

Tsutomu Kobayashi,* Masato Nozawa,† and Yu-ichi Takamizu‡
Department of Physics, Waseda University, Okubo 3-4-1, Shinjuku, Tokyo 169-8555, Japan

We study the emission of scalar fields into the bulk from a six-dimensional rotating black hole pierced by a 3-brane. We determine the angular eigenvalues in the presence of finite brane tension by using the continued fraction method. The radial equation is integrated numerically, giving the absorption probability (graybody factor) in a wider frequency range than in the preexisting literature. We then compute the power and angular momentum emission spectra for different values of the rotation parameter and brane tension, and compare their relative behavior in detail. As is expected from the earlier result for a nonrotating black hole, the finite brane tension suppresses the emission rates. As the rotation parameter increases, the power spectra are reduced at low frequencies due to the smaller Hawking temperature and are enhanced at high frequencies due to superradiance. The angular momentum spectra are enhanced over the whole frequency range as the rotation parameter increases. The spectra and the amounts of energy and angular momentum radiated away into the bulk are thus determined by the interplay of these effects.

PACS numbers: 04.50.-h, 04.70.Dy

I. INTRODUCTION

Braneworld models with large extra dimensions [1, 2, 3] bring us an interesting possibility to address the hierarchy problem by lowering the fundamental scale of gravity down to order of TeV. It has been argued in the context of TeV scale gravity that mini black holes might be created through high-energy particle collision at future colliders [4]. Much effort has been directed towards a theoretical understanding of the black hole formation at TeV energies (e.g., [5]). After their production, the black holes will decay via Hawking radiation [6]. This process provides a window to probe high-energy physics, gravity at small distances, and properties of extra dimensions, which motivates recent extensive studies on this topic. A nonexhaustive sampling of the literature can be found in Refs. [7, 8, 9, 10, 11, 12, 13, 14, 15, 16, 17, 18, 19, 20, 21, 22, 23, 24, 25, 26, 27]. For a review see Ref. [28]. Most of the related work to date has ignored the effect of brane tension, treating black holes as "isolated" ones (see, however, Refs. [29, 30, 31, 32] for the effects of self-gravity of branes).

It is in general very difficult to obtain a black hole solution localized on a brane with finite tension because tension curves the brane as well as the bulk (cf. Refs. [33, 34, 35, 36]). However, codimension-2 branes exceptionally allow for a simple construction of localized black holes thanks to their special property; starting from the Myers-Perry solution [37] one rescales the polar angle around a symmetry axis as $\psi \to B\psi$ and then the brane tension is proportional to the deficit angle $2\pi(1-B)$. In this way both nonrotating [38] and rotating [39] black holes on codimension-2 branes have been constructed. Following the work of [38], Hawking evaporation [40] and the quasi-normal modes for bulk scalars [41, 42] and fermions [43] have been investigated in the nonrotating background, showing that the finite brane tension modifies the standard result derived assuming negligible tension.

In this paper, we shall consider a six-dimensional *rotating* black hole pierced by a tense 3-brane and discuss the emission of massless scalar fields into the bulk. We intend to shed light on the spin-down phase in the life of a black hole, which is often neglected in the literature but could be of some significance. (In fact, a rotating black hole does not necessarily spin-down to zero, but evolves toward a nonzero angular momentum [44, 45].) Ignoring the brane tension, very recently Creek *et al.* studied the emission of scalars in the bulk in a higher-dimensional rotating black hole background [25]. They employed matching techniques to obtain an analytic solution to the scalar field equation, which is a good approximation in the low-energy ($\omega r_h \ll 1$) and slow-rotation ($a/r_h \ll 1$) regime, where ω is the energy of the emitted particle, r_h is the black hole horizon radius, and a is the rotation parameter. In the present paper, with the help of numerical computations we are able to handle the intermediate regime ($\omega r_h \gtrsim 1$ and $a/r_h \gtrsim 1$), and thus we not only include the effect of the finite tension but also extend the range of validity of [25].

This paper is organized as follows. In the next section we give a quick review of the rotating black hole solution on a codimension-2 brane. In Sec. III we present separated equations of motion for a massless scalar field and determine angular eigenvalues in the presence of the deficit angle. Then in Sec. IV the radial equation is solved numerically to give the power and angular momentum emission spectra. Finally we summarize our conclusions in Sec. V. Appendix contains the analytic calculation of the absorption probability, which complements the numerical results presented in the main text.

---

*Email: tsutomu"at"gravity.phys.waseda.ac.jp
†Email: nozawa"at"gravity.phys.waseda.ac.jp
‡Email: takamizu"at"gravity.phys.waseda.ac.jp

II. A ROTATING BLACK HOLE ON A CODIMENSION TWO BRANE

We begin with a brief review of the rotating black hole solution on a codimension-2 brane. (For further detail see Refs. [38, 39].) The solution shares some properties with the Myers-Perry black hole [37]. We are considering the models with five spatial dimensions, and so the rotation group is $SO(5)$. The number of Casimirs (i.e., the number of mutually commuting elements of the group) is equal to rank$[SO(5)] = 2$. Hence, we have two axes of rotation associated with two angular momenta. However, in the present article we will be focusing on the special but simple case of a single rotation parameter with the angular momentum pointing along the brane. This is indeed an interesting case from the phenomenological point of view, because the black hole formed by the collision of two particles confined to the brane will have a single rotation parameter. The exact metric that describes such a rotating black hole is given by [39]

$$\begin{aligned}\mathrm{d}s^2 = &-\left(1-\frac{\hat{\mu}}{r\rho^2}\right)\mathrm{d}t^2 - \frac{2\hat{\mu}a}{r\rho^2}\sin^2\theta\mathrm{d}t\mathrm{d}\phi + \frac{\rho^2}{\Delta}\mathrm{d}r^2 \\ &+\rho^2\mathrm{d}\theta^2 + \sin^2\theta\left(r^2+a^2+\frac{\hat{\mu}a^2}{r\rho^2}\sin^2\theta\right)\mathrm{d}\phi^2 \\ &+ r^2\cos^2\theta\left(\mathrm{d}\chi^2 + B^2\sin^2\chi\mathrm{d}\psi^2\right), \qquad (1)\end{aligned}$$

where

$$\Delta := r^2 + a^2 - \frac{\hat{\mu}}{r}, \quad \rho^2 := r^2 + a^2\cos^2\theta. \qquad (2)$$

The coordinate ranges are $0 \le \theta \le \pi/2$, $0 \le \chi \le \pi$, and $0 \le \phi, \psi < 2\pi$. The parameter B is related to the brane tension σ as

$$B = 1 - \frac{\sigma}{2\pi M_*^4}, \qquad (3)$$

where M_* is the six-dimensional fundamental scale. We assume that $0 < B \le 1$. When $B = 1$, the above metric reduces to the usual Myers-Perry solution with a single rotation parameter in six dimensions [37]. When $B \ne 1$ the solution is asymptotically conical. The parameters $\hat{\mu}\,(> 0)$ and a denote the specific mass and angular momentum, respectively, related to the ADM mass and angular momentum of the black hole as

$$M_{\rm BH} = 2A_4M_*^4\,\hat{\mu}\,B, \quad J_{\rm BH} = \frac{1}{2}M_{\rm BH}a, \qquad (4)$$

where $A_d = 2\pi^{(d+1)/2}/\Gamma[(d+1)/2]$ is the area of a unit d-sphere. Note here that the effect of the deficit angle B is separated out from the definition of the area. The black hole horizon radius r_h follows from $\Delta(r_h) = 0$. For later purpose it is convenient to define the dimensionless measure of the angular momentum $a_* := a/r_h$. Since the sign flip $a \to -a$ simply changes the direction of rotation, in what follows we will assume $a \ge 0$ without any loss of generality.

Note that $\Delta(r_h) = 0$ has a root for arbitrary a. This should be contrasted with the four-dimensional Kerr black hole, which has an upper bound on the rotation parameter. This point will become clearer by considering the black hole temperature. The generator of the horizon is parallel to the Killing vector $\xi^\mu = (\partial/\partial t)^\mu + \Omega_h(\partial/\partial\phi)^\mu$, and the surface gravity of the black hole is given by $\kappa^2 = -(\nabla^\mu\xi^\nu)(\nabla_\mu\xi_\nu)/2$. Here Ω_h is the angular velocity of the horizon:

$$\Omega_h := \frac{a}{r_h^2 + a^2}. \qquad (5)$$

Then, the Hawking temperature is given by [6]

$$T_H := \frac{\kappa}{2\pi} = \frac{3 + a_*^2}{4\pi(1+a_*^2)r_h}, \qquad (6)$$

and one sees that the temperature never attains zero. This means the black hole is manifestly nondegenerate for any value of a.

An interesting effect of the brane tension perhaps one is immediately aware of is the rescaling of the gravitational scale $M_* \to M_{*\rm eff} = B^{1/4}M_*$, as is observed in Eq. (4). This modifies the scenario of the black hole production and evaporation as follows [38, 39, 40]. Suppose that a black hole is formed through a particle collision and its mass $M_{\rm BH}$ is fixed by the accelerator. The upper limit on the impact parameter b is given by $b \le 2r_h$. Since $r_h \sim M_{\rm BH}^{1/3}/M_{*\rm eff}^{4/3}$, for fixed $M_{\rm BH}$ the horizon radius is *larger* than the naive estimate, $r_h \sim B^{-1/3}$, which is called the "lightning rod" effect [38, 39]. In the present situation producing black holes will become easier due to this effect. Since the black hole formed in this way has the angular momentum $J = bM_{\rm BH}/2$, we have $J \le J_{\rm max} := M_{\rm BH}r_h$, and so the angular momentum can also be *larger* than naively expected, $J_{\rm max} \sim B^{-1/3}$. Now the time scale τ of mass loss is estimated from $\mathrm{d}M_{\rm BH}/\mathrm{d}t \sim$ (horizon area)$\times T_H^6 \sim Br_h^{-2}$, yielding $\tau \sim B^{-5/3}$. Thus the lifetime of the black hole will become longer. Similarly, the time scale τ' of angular momentum loss is estimated roughly from $\mathrm{d}J_{\rm BH}/\mathrm{d}t \sim r_h\mathrm{d}M_{\rm BH}/\mathrm{d}t$. This gives $\tau' \sim B^{-5/3}$, and hence the time scale τ' will also become larger.

The above mentioned modifications are caused by the rescaling of the gravitational scale. In the rest of the paper we separate this effect and discuss the impact of finite brane tension on Hawking emission *with the horizon radius r_h fixed.*

Let us finally remark that in models with extra dimensions the bulk will be compact. Throughout the paper we assume that the horizon size of the black hole is smaller than the typical compactification scale. With this, the above solution provides a nice description of a six-dimensional black hole localized on a 3-brane.

III. SCALAR WAVE EQUATION IN A ROTATING BLACK HOLE BACKGROUND

We now turn to discuss Hawking emission of massless scalar fields. To this end we solve the equation of motion for a massless scalar field Ψ in the rotating black hole background (1). The governing equation is given by

$$\frac{1}{\sqrt{-g}}\partial_\mu\left(\sqrt{-g}\, g^{\mu\nu}\partial_\nu\Psi\right)=0, \tag{7}$$

where $\sqrt{-g}=B\rho^2r^2\sin\theta\cos^2\theta\sin\chi$. We can separate the above equation by assuming the ansatz

$$\Psi=e^{-i\omega t}e^{im\phi}R(r)S(\theta)T(\chi)\Xi(\psi), \tag{8}$$

where $m=0,\pm1,\pm2,...$ The radial equation is

$$\frac{1}{r^2}\frac{\mathrm{d}}{\mathrm{d}r}\left(r^2\Delta\frac{\mathrm{d}}{\mathrm{d}r}R\right)+\left[\frac{K^2}{\Delta}-\nu(\nu+1)\frac{a^2}{r^2}-\lambda\right]R=0, \tag{9}$$

where

$$K:=(r^2+a^2)\omega-am, \quad \lambda:=\eta+a^2\omega^2-2am\omega, \tag{10}$$

and the angular equations are given by

$$\frac{1}{\sin\theta\cos^2\theta}\frac{\mathrm{d}}{\mathrm{d}\theta}\left(\sin\theta\cos^2\theta\frac{\mathrm{d}}{\mathrm{d}\theta}S\right)+\left[a^2\omega^2\cos^2\theta-\frac{m^2}{\sin^2\theta}-\frac{\nu(\nu+1)}{\cos^2\theta}\right]S=-\eta S, \tag{11}$$

$$\frac{1}{\sin\chi}\frac{\mathrm{d}}{\mathrm{d}\chi}\left(\sin\chi\frac{\mathrm{d}}{\mathrm{d}\chi}T\right)-\frac{\mu^2}{\sin^2\chi}T=-\nu(\nu+1)T, \tag{12}$$

$$\frac{1}{B^2}\frac{\mathrm{d}^2}{\mathrm{d}\psi^2}\Xi=-\mu^2\Xi. \tag{13}$$

Here $\eta,\nu,$ and μ are separation constants. The above equations of motion are the same as those derived in Ref. [16] except that in the last equation (13) there appears "B." We immediately see that

$$\mu=\frac{n}{B} \quad \text{with} \quad n=0,\pm1,\pm2,... \tag{14}$$

As is emphasized in Ref. [40], the eigenvalues are coupled and therefore all of the eigenvalues will be modified when $B\neq1$. Since the eigenvalues ν and η will be dependent on $|n|$, we can restrict to $n\geq0$ without any loss of generality. Negative values of n can be treated similarly.

We proceed to determine the eigenvalue ν. Performing the change of the variable and function as $x=\cos\chi$, $\mathcal{T}:=(1-x^2)^{-\mu/2}T$, we have

$$(1-x^2)\frac{\mathrm{d}^2}{\mathrm{d}x^2}\mathcal{T}-2(\mu+1)x\frac{\mathrm{d}}{\mathrm{d}x}\mathcal{T}+(\nu-\mu)(\nu+\mu+1)\mathcal{T}=0. \tag{15}$$

The boundary conditions are given by

$$\frac{\mathrm{d}}{\mathrm{d}x}\mathcal{T}=\pm\frac{(\nu-\mu)(\nu+\mu+1)}{2(\mu+1)}\mathcal{T} \quad \text{at} \quad x=\pm1. \tag{16}$$

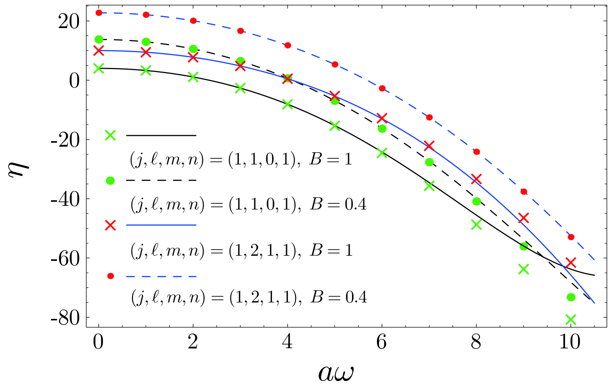

FIG. 1: Eigenvalue η for selected values of (j,ℓ,m,n) and B. Solid and dashed lines refer to the series expansion (28) truncated at 7th order, while points and crosses show the numerical results without relying on the small-$a\omega$ expansion.

As in [42], we first consider the special case in which $B=1/N$ with $N=1,2,...$ and hence $\mu=nN$ is an integer. In this case it is easy to find $\nu=\mu,\mu+1,\mu+2,...$ Thus the eigenvalue ν can be written in terms of an integer j as

$$\nu=j+b_n, \quad b_n:=\frac{1-B}{B}|n|, \tag{17}$$

where $j\geq|n|$ and the absolute value signs are inserted for clarity. Although Eq. (17) was derived for $B^{-1}=1,2,...,$ this result can be generalized to arbitrary $B\in(0,1]$ [42]. We have confirmed numerically that Eq. (17) indeed holds for noninteger values of B^{-1}.

When $B=1$, ν is independent of n (and as a result η is also independent of n). For the tensional case, however, ν depends on n (and hence does η). From Eq. (17) we see that the brane tension *increases* the eigenvalue ν relative to the tensionless case.

To determine the eigenvalue η, we exploit the continued fraction method developed originally by Leaver [46]. Following [47], we write $S=(1-u^2)^{|m|/2}u^\nu\mathcal{S}$ with $u=\cos\theta$. Then, $\mathcal{S}$ obeys

$$(1-u^2)\frac{\mathrm{d}^2}{\mathrm{d}u^2}\mathcal{S}+2\left[(\nu+1)\frac{1-u^2}{u}-(|m|+1)u\right]\frac{\mathrm{d}}{\mathrm{d}u}\mathcal{S}+\left[a^2\omega^2u^2+\eta-\nu(\nu+3)-|m|(|m|+2\nu+3)\right]\mathcal{S}=0, \tag{18}$$

subject to the regularity boundary conditions

$$\frac{\mathrm{d}}{\mathrm{d}u}\mathcal{S}=0 \qquad \text{at} \quad u=0, \tag{19}$$

$$\frac{\mathrm{d}}{\mathrm{d}u}\mathcal{S}=\frac{a^2\omega^2+\eta-\nu(\nu+3)-|m|(|m|+2\nu+3)}{|m|+1}\mathcal{S} \qquad \text{at} \quad u=1. \tag{20}$$

We seek for a series solution in the form of

$$\mathcal{S}=\sum_{p=0}^{\infty}a_pu^{2p}. \tag{21}$$

Substituting this to Eq. (18) we obtain the three-term recursion relation

$$\alpha_0 a_1 + \beta_0 a_0 \ = \ 0, \tag{22}$$

$$\alpha_p a_{p+1} + \beta_p a_p + \gamma_p a_{p-1} \ = \ 0, \quad p = 1, 2, ..., \tag{23}$$

where

$$\alpha_p \ := \ 2(p+1)(2\nu + 2p + 3), \tag{24}$$

$$\beta_p \ := \ \eta - (\nu + |m| + 2p)(\nu + |m| + 2p + 3), \tag{25}$$

$$\gamma_p \ := \ (a\omega)^2. \tag{26}$$

The continued fraction equation for the eigenvalue is then given by

$$\beta_0 - \cfrac{\alpha_0\gamma_1}{\beta_1 - \cfrac{\alpha_1\gamma_2}{\beta_2 - \cfrac{\alpha_2\gamma_3}{\beta_3 - \cdots}}} = 0. \tag{27}$$

The boundary conditions are automatically satisfied by the series solution (21).

We expand the eigenvalue η in powers of $a\omega$ around $a\omega = 0$:

$$\eta = \sum_{p=0}^{\infty} \tilde{\eta}_p (a\omega)^p. \tag{28}$$

In order for the series to converge in the limit $a\omega \to 0$, we require that it has a finite number of terms. Imposing $\beta_q = 0$ for some integer $q \geq 0$ and identifying $2q = \ell - (j + |m|)$, we obtain

$$\eta = (\ell + b_n)(\ell + 3 + b_n) \tag{29}$$

for $a\omega = 0$. Here we have a restriction for the integer ℓ:

$$\frac{1}{2}(\ell - j - |m|) = 0, 1, 2, ... \tag{30}$$

To determine the coefficients in (28) it is convenient to use the qth inversion of (27):

$$\beta_q - \cfrac{\alpha_{q-1}\gamma_q}{\beta_{q-1} - \cfrac{\alpha_{q-2}\gamma_{q-1}}{\beta_{q-2} - \cdots}} = \cfrac{\alpha_q \gamma_{q+1}}{\beta_{q+1} - \cfrac{\alpha_{q+1}\gamma_{q+2}}{\beta_{q+2} - \cdots}}. \tag{31}$$

With some manipulation we find $\tilde{\eta}_1 = \tilde{\eta}_3 = 0$ and

$$\tilde{\eta}_0 \ = \ (\ell + b_n)(\ell + 3 + b_n), \tag{32}$$

$$\tilde{\eta}_2 \ = \ -\frac{2\ell(\ell+3) + 3 + 2j + 2j^2 - 2m^2 + 4(\ell + j + 2)b_n + 4b_n^2}{[2(\ell + b_n) + 1][2(\ell + b_n) + 5]}, \tag{33}$$

$$\begin{aligned}\tilde{\eta}_4 \ = \ & \frac{(\ell - j - |m|)(\ell + j - |m| + 1 + 2b_n)}{4[2(\ell + b_n) + 1]^2}\left[\frac{(\ell - j - |m| - 2)(\ell + j - |m| - 1 + 2b_n)}{4[2(\ell + b_n) - 1]} - \tilde{\eta}_2\right] \\ & - \frac{(\ell - j - |m| + 2)(\ell + j - |m| + 3 + 2b_n)}{4[2(\ell + b_n) + 5]^2}\left[\frac{(\ell - j - |m| + 4)(j + \ell - |m| + 5 + 2b_n)}{4[2(\ell + b_n) + 7]} + \tilde{\eta}_2\right].\end{aligned} \tag{34}$$

One can confirm that Eqs. (32)–(34) correctly reproduce the known result in the case of $b_n = 0$ [25, 47].[1] Although the expressions are too lengthy, higher order coefficients can be obtained easily.

One can instead integrate Eq. (11) numerically to determine η. The numerical computation has an advantage that it does not rely on the small-$a\omega$ expansion. In Fig. 1 we compare the series expansion truncated at 7th order with the numerical result that is free from any approximation. It can be seen from this that the analytic result can reproduce the numerical computation remarkably well even for $a\omega \sim 6$. Therefore, in the next section we will safely use the analytic approximation for η. We thus avoid numerical determination of the eigenvalues and so the rest of the problem simply reduces to solving the ordinary differential equation for the radial mode function.

We remark here that while the brane tension does not affect the $n = 0$ mode, the eigenvalue η (for $n \neq 0$) increases as B decreases (and so the tension increases), as can be seen from Fig. 1. This behavior has been observed for a nonrotating black hole in [40], and now it turns out that the similar thing generally holds for a rotating one.

---

[1] The second order coefficient in [47] contains a sign error, which has been corrected in [25].

IV. POWER AND ANGULAR MOMENTUM EMISSION SPECTRA

We are going to solve the radial equation (9) to compute the emission spectra. To do so we first specify the asymptotic form of the solution close to the horizon and far away from it. In terms of the new coordinate defined by $\mathrm{d}r_* := [(r^2+a^2)/\Delta]\mathrm{d}r$ and the function $\Phi := r(r^2+a^2)^{1/2}R$, Eq. (9) can be rewritten as

$$\frac{\mathrm{d}^2}{\mathrm{d}r_*^2}\Phi + \left\{[\omega - m\Omega(r)]^2 - V(r)\right\}\Phi = 0. \tag{35}$$

where $\Omega(r) := a/(r^2+a^2)$ and

$$\begin{aligned} V(r) :=& \frac{\Delta}{(r^2+a^2)^2}\left[\lambda + \nu(\nu+1)\frac{a^2}{r^2}\right] \\ &+ \frac{1}{r(r^2+a^2)^{1/2}}\frac{\mathrm{d}^2}{\mathrm{d}r_*^2}\left[r(r^2+a^2)^{1/2}\right]. \end{aligned} \tag{36}$$

It is easy to see that $V(r) \approx 0$ as $r \to r_h$ and $r \to \infty$. Keeping this in mind the asymptotic solutions are found to be

$$r \to r_h: \quad R \simeq A_{\mathrm{in}}^{(h)} e^{-iky} + A_{\mathrm{out}}^{(h)} e^{iky}, \tag{37}$$

$$r \to \infty: \quad R \simeq A_{\mathrm{in}}^{(\infty)} \frac{e^{-i\omega r}}{r^2} + A_{\mathrm{out}}^{(\infty)} \frac{e^{i\omega r}}{r^2}, \tag{38}$$

where

$$k := \omega - m\Omega_h, \tag{39}$$

and y is the tortoise-like coordinate defined by

$$y := \frac{1+a_*^2}{3+a_*^2} r_h \ln\left[\frac{\Delta(r)}{r^2+a^2}\right]. \tag{40}$$

We choose the boundary condition $A_{\mathrm{out}}^{(h)} = 0$, i.e., we impose that no outgoing modes exist near the horizon. The absorption probability is then given by

$$|\mathcal{A}_{j\ell mn}|^2 = 1 - \left|\frac{A_{\mathrm{out}}^{(\infty)}}{A_{\mathrm{in}}^{(\infty)}}\right|^2. \tag{41}$$

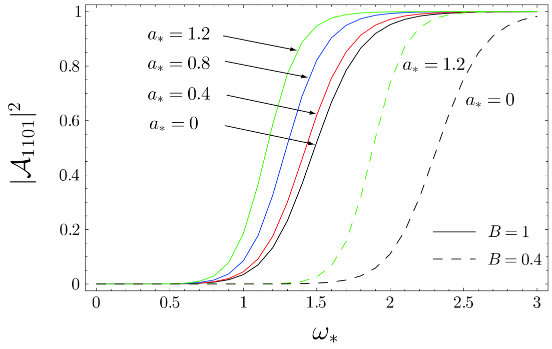

FIG. 2: Absorption probabilities for $(j, \ell, m, n) = (1, 1, 0, 1)$, $B = 1, 0.4$, and various a_*.

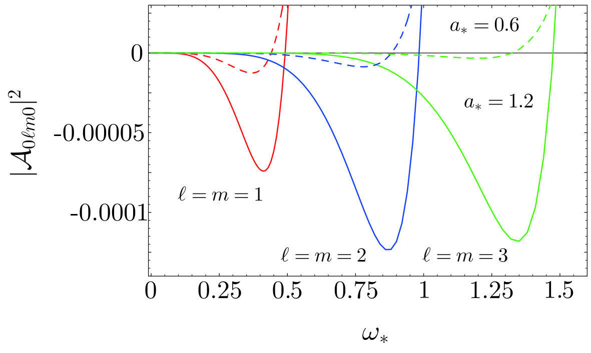

FIG. 3: Superradiance modes for $a_* = 1.2$ and 0.6. The absorption probabilities are negative for $\omega_* < m\Omega_h r_h$, where $\Omega_h r_h \simeq 0.49$ for $a_* = 1.2$ and $\Omega_h r_h \simeq 0.44$ for $a_* = 0.6$.

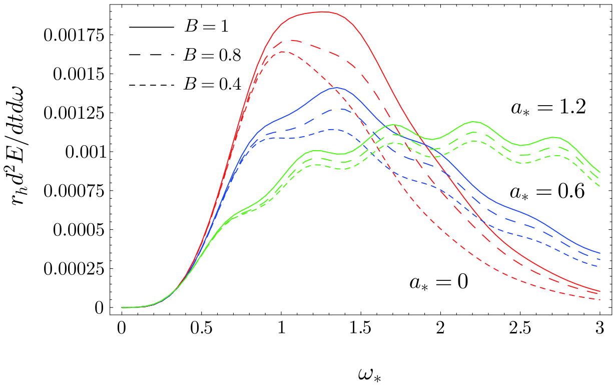

FIG. 4: Power emission spectra for different values of a_* and B.

Note the explicit dependence on the angular eigenvalue n of the absorption probability. This is due to the nonzero brane tension ($B \neq 1$).

Using the series expansion of the eigenvalue η (truncated at 7th order), we numerically integrate Eq. (9) and compute the absorption probability. We defer to Appendix the analytic calculation of the absorption probability in the limit $\omega_* := \omega r_h \ll 1$ and $a_* \ll 1$. The analytic and numerical results are found to be in good agreement in the regime $\omega_* \ll 1$ and $a_* \ll 1$.

As was remarked above, both η and ν become larger as the brane tension increases. This results in the enhancement of the "potential" (36), which will reduce the absorption probability. A typical example of the absorption probability (as a function of ω_*) is plotted for various a_* and B in Fig. 2, showing that the absorption probability indeed decreases with decreasing B. We can see in Fig. 3 that there appear superradiant modes with $0 < \omega < m\Omega_h$, for which the absorption probability is negative [48].

From the absorption probability we compute the energy and angular momentum emission rates. They are

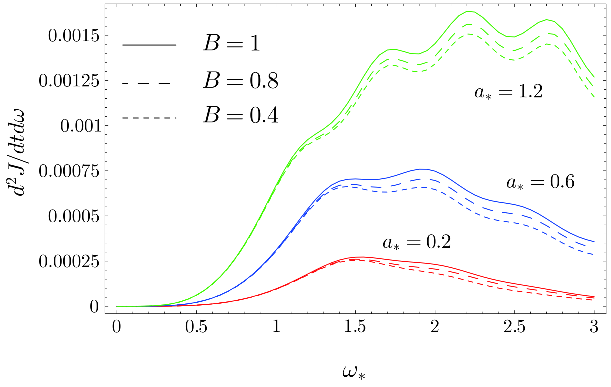

FIG. 5: Angular momentum spectra for different values of a_* and B.

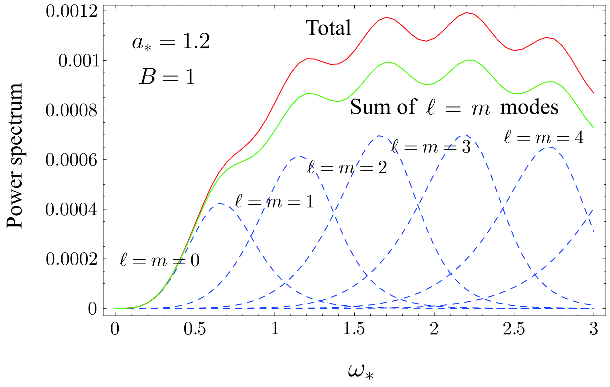

FIG. 6: Contributions from $\ell = m$ modes. Red (solid) line shows the total power emission spectrum depicted also in Fig. 4, while green (solid) line represents the sum of $\ell = m$ modes, each of which is shown by blue (dashed) line.

given by the formulas

$$\frac{\mathrm{d}^2E}{\mathrm{d}t\mathrm{d}\omega} = \frac{1}{2\pi}\sum_{j,\ell,m,n}\frac{\omega}{e^{k/T_H}-1}\left|\mathcal{A}_{j\ell mn}\right|^2, \tag{42}$$

$$\frac{\mathrm{d}^2J}{\mathrm{d}t\mathrm{d}\omega} = \frac{1}{2\pi}\sum_{j,\ell,m,n}\frac{m}{e^{k/T_H}-1}\left|\mathcal{A}_{j\ell mn}\right|^2, \tag{43}$$

where T_H and k were already defined in Eqs. (6) and (39), respectively. We summed up to $\ell = 5$ modes in calculating the above quantities. Our numerical results are summarized in Figs. 4 and 5.

We find that the finite brane tension reduces the power and angular momentum emission spectra. This is anticipated from the behavior of the absorption probability stated above. The power emission rates are reduced in the low frequency regime as the rotation parameter a_* increases. This is because the Hawking temperature becomes lower with increasing a_*. However, the power emission rates are enhanced at high frequencies. This should be caused by superradiance. The angular momentum emission rates are enhanced over the whole frequency range with increasing a_* because the effects of superradiance win out. (In the previous estimates [44, 45, 49] significant superradiance is observed as the angular momentum increases.) One can see from Fig. 6 that a large portion of the contribution to the power emission spectrum is coming from the $\ell = m$ modes, which show the superradiant behavior (except for $\ell = m = 0$). We confirmed that the same is true for the angular momentum spectrum. As a_* increases the amplitudes of these modes are enhanced, lifting up the total spectra. One can also see that the oscillatory behavior of the spectra is due to these modes, with each peak corresponding to each mode. However, the above things do not mean that only the $\ell = m$ modes are important in determining the behavior of the spectra; the eigenvalues for the $\ell = m$ modes are independent of the conical deficit and the other modes ($|n| \geq 1$) determine the decrease in the spectra with decreasing B.

Since the brane induced metric is the same as the tensionless case, the Hawking spectrum of brane-localized fields does not depend on the tension (for fixed r_h).[2] The emission of brane scalar fields has been studied in Refs. [10, 11, 13, 21, 22] for rotating black holes in various dimensions, and the brane-to-bulk ratio of the energy emission rates has been discussed in [25], implying that the dominant channels are the brane-localized modes. Since the finite brane tension further suppresses the bulk field contributions, it is likely that brane-localized scalar emission dominates bulk emission also in the present case. Although bulk modes will not be observed directly, bulk emission is still important because it indirectly determines the amount of energy and angular momentum left for brane-localized emission.

V. CONCLUDING REMARKS

The black hole production in TeV scale gravity offers us a possible window to explore the presence of extra dimensions. In this paper we have studied Hawking emission of scalar fields into the bulk from a rotating black hole localized on a codimension-2 brane. The exact solution we used is a rare example in which we can treat self-gravity of the brane consistently in the context of brane-localized black holes [39]. This simple model enables us to elucidate how the brane tension modifies the Hawking spectra relative to the tensionless case.

Assuming the separable ansatz for the scalar field, we have determined the angular eigenvalue in the series expansion form: $\eta = \tilde{\eta}_0 + \tilde{\eta}_2(a\omega)^2 + \cdots$. This analytic approximation (truncated at 7th order) was turned out to be in excellent agreement with the numerical result in the regime $a\omega \lesssim 6$. Using the analytic form of η, we then integrated the radial equation numerically and computed the power and angular momentum emission spectra. Our finding is that the finite brane tension suppresses the power and angular momentum spectra. We also showed that the power emission rates are reduced at low frequencies and enhanced at high frequencies as the rotation parameter a_* increases. The suppression at low frequencies is due to the smaller Hawking temperature and the enhancement at high frequencies is caused by superradiance. The angular momentum emission rates are enhanced over the whole frequency range as a_* increases due to superradiance. The spectra and the amounts of energy and angular momentum radiated away into the bulk are thus determined by the interplay of these effects. To conclude, the brane tension plays an important role in the evaporation process in the life of a mini black hole.

---

[2] Although this statement is true in the present model, it is not clear whether or not the induced metric is independent of the brane tension in more realistic situations with compact extra dimensions.

It is possible to obtain an analytic but approximate solution to the radial equation, as has been done recently in [25] and is replicated in Appendix. The range of validity of this analytic approximation is restricted to $\omega_* \ll 1$ and $a_* \ll 1$. Therefore, even in the tensionless case ($B = 1$) our result is new, in that we have extended the range of validity of [25] by invoking the numerical approach. We however exploited the analytic expression for η to simplify numerical calculations. The eigenvalues η obtained here by the continued fraction method are quite accurate even for $a_*\omega_* \sim 6$, which allows us to compute the spectra for $\omega_* \gtrsim 1$ and $a_* \gtrsim 1$. In order to explore the full regime extending to $a\omega \gtrsim \mathcal{O}(10)$, we need to solve both the radial and angular equations numerically, which is left to further investigation.

In this paper we considered only the emission of scalar fields. It would be interesting to study the bulk emission of higher spin fields and determine the brane-to-bulk ratio of the energy and angular momentum emission rates. Recently, it has been reported that for fermion fields the bulk emission dominates the brane-localized emission in a six- or higher dimensional Schwarzschild background [27]. Therefore, investigating the effects of the finite brane tension [43] and the black hole rotation on the fermion emission would be of particular interest. Another open issue is to clarify the spin-down evolution of the rotating black hole and the effect of brane tension on it. This process can be studied along the line of [44, 45]. We plan to return to this issue in the near future. Finally, it is fair to say that all of the results in this paper have been derived ignoring the compactification mechanism, which may affect both brane and bulk emissions. This point is worth exploring, though constructing brane-localized black hole solutions in compact space will be quite difficult.

Acknowledgments

We would like to thank Sam Dolan and Marc Casals for useful comments. TK, MN, and YT are supported by the JSPS under Contract Nos. 19-4199, 19-204, and 17-53192.

APPENDIX A: ANALYTIC APPROXIMATION METHOD FOR $\omega_* \ll 1$ AND $a_* \ll 1$

In this appendix we present an approximation method to obtain an analytic expression for the absorption probability. Our result here simply generalizes that of [25] to include the deficit angle (see also [13]). The procedure is as follows: first we obtain the asymptotic solutions in the far-field and near-horizon regions, and then match the two solutions in the intermediate zone. The approximation is valid in the low-energy ($\omega_* \ll 1$) and slow-rotation ($a_* \ll 1$) regime. We check that in this range the analytic result agrees with the numerical one displayed in the main text.

Let us first focus on the near-horizon zone ($r \simeq r_h$). It is convenient to work with a new radial variable defined by

$$\xi := \frac{\Delta}{r^2 + a^2}, \tag{A1}$$

for which we have

$$\frac{\mathrm{d}\xi}{\mathrm{d}r} = \frac{(1-\xi) r A(r)}{r^2 + a^2} \tag{A2}$$

with $A(r) := 3 + a^2/r^2$. Now the horizon is located at $\xi = 0$, while the asymptotic infinity corresponds to $\xi = 1$. Near the horizon, the radial equation (9) reduces to

$$\begin{aligned} &\xi(1-\xi)\frac{\mathrm{d}^2 R}{\mathrm{d}\xi^2} + (1-\gamma\xi)\frac{\mathrm{d}R}{\mathrm{d}\xi} \\ &\qquad + \left[\frac{K_*^2}{\xi(1-\xi)A_*^2} - \frac{\Lambda_*(1+a_*^2)}{(1-\xi)A_*^2}\right] R = 0, \end{aligned} \tag{A3}$$

where

$$\begin{aligned} &A_*^2 := 3 + a_*^2, \quad K_* := (1+a_*^2)\omega_* - a_* m, \\ &\gamma := 1 - 4a_*^2/A_*^2, \quad \Lambda_* := \lambda + \nu(\nu+1)a_*^2. \end{aligned}$$

Performing the transformation $R = \xi^\alpha (1-\xi)^\beta F(\xi)$ with

$$\alpha = -i\frac{K_*}{A_*}, \tag{A4}$$

$$\beta = 1 - \frac{\gamma}{2} - \sqrt{\left(1-\frac{\gamma}{2}\right)^2 - \frac{K_*^2 - \Lambda_*(1+a_*^2)}{A_*^2}}, \tag{A5}$$

we obtain a hypergeometric differential equation

$$\xi(1-\xi)\frac{\mathrm{d}^2 F}{\mathrm{d}\xi^2} + \left[\tilde{c} - (1+\tilde{a}+\tilde{b})\xi\right]\frac{\mathrm{d}F}{\mathrm{d}\xi} - \tilde{a}\tilde{b}F = 0, \tag{A6}$$

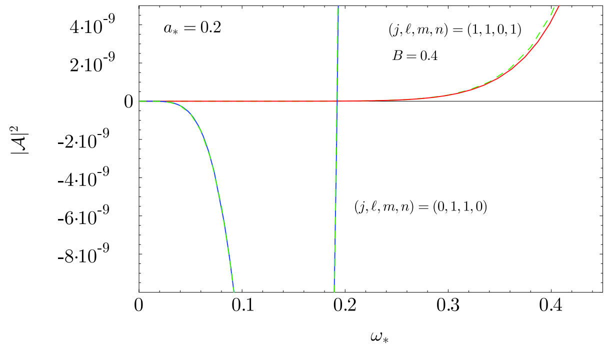

FIG. 7: Absorption probabilities computed analytically and numerically. Solid lines follow from the analytic approximation, while dashed lines denote our numerical result.

where $\tilde{a} := \alpha + \beta + \gamma - 1$, $\tilde{b} := \alpha + \beta$, and $\tilde{c} = 1 + 2\alpha$. Thus, the near-horizon solution is given in terms of the hypergeometric function by

$$\begin{aligned} R =& A_- \xi^{\alpha} (1-\xi)^{\beta} F(\tilde{a}, \tilde{b}, \tilde{c}; \xi) \\ &+ A_+ \xi^{-\alpha} (1-\xi)^{\beta} F(\tilde{a} - \tilde{c} + 1, \tilde{b} - \tilde{c} + 1, 2 - \tilde{c}; \xi), \end{aligned} \tag{A7}$$

where $A_\pm$ are integration constants. In the limit $r \to r_h$ ($\xi \to 0$) we have

$$R \simeq A_- \xi^{\alpha} + A_+ \xi^{\alpha} = A_- e^{-iky} + A_+ e^{iky}, \tag{A8}$$

where y is defined earlier in the main text. Since we are imposing the boundary condition such that no outgoing wave is present at the horizon, we set $A_+ = 0$. Thus we arrive at

$$R_{\rm NH} = A_- \xi^{\alpha} (1-\xi)^{\beta} F(\tilde{a}, \tilde{b}, \tilde{c}; \xi) \quad \text{at} \quad r \simeq r_h. \tag{A9}$$

One can check that the convergence condition for the hypergeometric function, $\mathrm{Re}[\tilde{c} - \tilde{a} - \tilde{b}] > 0$, is indeed satisfied.

Now we extend the solution (A9) to go beyond the near-horizon zone. Using the formula

$$\begin{aligned} F(\tilde{a}, \tilde{b}, \tilde{c}; \xi) =& \frac{\Gamma(\tilde{c})\Gamma(\tilde{c} - \tilde{a} - \tilde{b})}{\Gamma(\tilde{c} - \tilde{a})\Gamma(\tilde{c} - \tilde{b})} \\ &\times F(\tilde{a}, \tilde{b}, \tilde{a} + \tilde{b} - \tilde{c} + 1; 1 - \xi) \\ &+ (1-\xi)^{\tilde{c} - \tilde{a} - \tilde{b}} \frac{\Gamma(\tilde{c})\Gamma(\tilde{a} + \tilde{b} - \tilde{c})}{\Gamma(\tilde{a})\Gamma(\tilde{b})} \\ &\times F(\tilde{c} - \tilde{a}, \tilde{c} - \tilde{b}, \tilde{c} - \tilde{a} - \tilde{b} + 1; 1 - \xi), \end{aligned}$$

and taking the limit $r \to \infty$ ($\xi \to 1$) we obtain

$$R_{\rm NH} \simeq A_1 r^{-3\beta} + A_2 r^{-3(2-\gamma-\beta)}, \tag{A10}$$

where

$$\begin{aligned} A_1 &:= A_- (1 + a_*^2)^{\beta} r_h^{3\beta} \frac{\Gamma(\tilde{c})\Gamma(\tilde{c} - \tilde{a} - \tilde{b})}{\Gamma(\tilde{c} - \tilde{a})\Gamma(\tilde{c} - \tilde{b})}, \\ A_2 &:= A_- (1 + a_*^2)^{2-\gamma-\beta} r_h^{3(2-\gamma-\beta)} \frac{\Gamma(\tilde{c})\Gamma(\tilde{a} + \tilde{b} - \tilde{c})}{\Gamma(\tilde{a})\Gamma(\tilde{b})}. \end{aligned} \tag{A11}$$

The expression (A10) should be matched to the far-field solution which will be derived below.

Let us go on to the far-field solution. In the far-field zone ($r \gg r_h$) the radial equation (9) reduces to

$$\frac{\mathrm{d}^2 R}{\mathrm{d}r^2} + \frac{4}{r}\frac{\mathrm{d}R}{\mathrm{d}r} + \left(\omega^2 - \frac{\eta}{r^2}\right) R = 0. \tag{A12}$$

The solution is given by

$$R_{\rm FF} = B_1 \frac{J_\tau(\omega r)}{r^{3/2}} + B_2 \frac{Y_\tau(\omega r)}{r^{3/2}}, \tag{A13}$$

where J_τ (Y_τ) is the Bessel function of the first (second) kind, $\tau := \sqrt{\eta + 9/4}$, and $B_{1,2}$ are the integration constants. This solution is in turn to be extended to the near-horizon zone. Taking the limit $\omega r \ll 1$ we get

$$R_{\rm FF} \simeq \frac{B_1}{r^{3/2}\Gamma(\tau+1)} \left(\frac{\omega r}{2}\right)^{\tau} - \frac{B_2 \Gamma(\tau)}{r^{3/2}\pi} \left(\frac{\omega r}{2}\right)^{-\tau}. \tag{A14}$$

The two solutions (A10) and (A14) appear to have different powers in r, but by taking the low-energy ($\omega_* \ll 1$) and slow-rotation ($a_* \ll 1$) limit we are able to match them. Neglecting terms of order ω_*^2, a_*^2, and $a_*\omega_*$, we have $A_* \simeq 3$, $\gamma \simeq 1$, and $\beta \simeq -(\ell + b_n)/3$, leading to $-3\beta \simeq \ell + b_n$ and $-3(2 - \gamma - \beta) \simeq -(\ell + b_n + 3)$ in Eq. (A10), where we used $\eta = (\ell + b_n)(\ell + b_n + 3) + \mathcal{O}(a_*^2\omega_*^2)$. As for Eq. (A14), we have $\tau - 3/2 \simeq \ell + b_n$ and $-(\tau + 3/2) \simeq -(\ell + b_n + 3)$. Thus in this limit we achieve exact matching.

The absorption probability can be expressed in terms of the ratio of the coefficients $B_r := B_1/B_2$. One finds

$$\begin{aligned} B_r =& -\frac{1}{\pi} \left[\frac{\omega_*(1 + a_*^2)^{1/3}}{2}\right]^{-(2\ell + 2b_n + 3)} \\ &\times \frac{\tau \Gamma^2(\tau)\Gamma(\tilde{a})\Gamma(\tilde{b})\Gamma(\tilde{c} - \tilde{a} - \tilde{b})}{\Gamma(\tilde{c} - \tilde{a})\Gamma(\tilde{c} - \tilde{b})\Gamma(\tilde{a} + \tilde{b} - \tilde{c})}. \end{aligned} \tag{A15}$$

In the limit $r \to \infty$ the solution (A13) can be written as

$$R_{\rm FF} \simeq A_{\rm in}^{(\infty)} \frac{e^{-i\omega r}}{r^2} + A_{\rm out}^{(\infty)} \frac{e^{i\omega r}}{r^2}, \tag{A16}$$

where

$$A_{\rm in}^{(\infty)} = (B_1 + iB_2) \frac{e^{i(\tau\pi/2 + \pi/4)}}{\sqrt{2\pi\omega}} \tag{A17}$$

$$A_{\rm out}^{(\infty)} = (B_1 - iB_2) \frac{e^{-i(\tau\pi/2 + \pi/4)}}{\sqrt{2\pi\omega}}. \tag{A18}$$

The absorption probability is given by $|\mathcal{A}|^2 = 1 - |A_{\rm out}^{(\infty)}/A_{\rm in}^{(\infty)}|^2$. In the low energy limit ($\omega_* \ll 1$) we have $B_r B_r^* \gg (B_r - B_r^*)/i \gg 1$. Hence,

$$|\mathcal{A}|^2 \simeq 2i \left(\frac{1}{B_r} - \frac{1}{B_r^*}\right). \tag{A19}$$

Substituting (A15) to (A19) results in a lengthy expression, but when m is not large we may expand the equation with respect to α ($\ll 1$) in the low-energy and slow-rotation regime. Then, at leading order in $\alpha = -iK_*/A_*$, one finds

$$|\mathcal{A}|^2 = \frac{4\pi K_*}{A_*} \frac{\Gamma^2(2\beta+\gamma-2)\Gamma^2(1-\beta)(2-2\beta-\gamma)\sin^2[\pi(2\beta+\gamma)]}{(\ell+b_n+3/2)\Gamma^2(\ell+b_n+3/2)\Gamma^2(\beta+\gamma-1)\sin^2[\pi(\beta+\gamma)]} \left[\frac{\omega_*(1+a_*^2)^{1/3}}{2}\right]^{2\ell+2b_n+3} . \tag{A20}$$

In Fig. 7 we compare this analytic result with our numerical calculation employed in the main text. It can be seen that the numerical result indeed agrees with the analytic one in the low-energy and slow-rotation regime. Since all the terms except K_* on the right hand side of Eq. (A20) are positive, the sign of $|\mathcal{A}|^2$ is controlled by $K_* = (1+a_*^2)\omega_* - a_* m = r_h(1+a_*^2)(\omega - m\Omega_h)$. Therefore, the absorption probability is negative for superradiant modes ($0 < \omega < m\Omega_h$).

In the low energy regime the $j = \ell = m = n = 0$ mode will be dominant, for which the absorption probability is given by

$$|\mathcal{A}_{0000}|^2 = \frac{4\omega_*^4(1+a_*^2)^2}{3(3+a_*^2)(2-\gamma)} + \cdots . \tag{A21}$$

This does not depend on the deficit angle.

To obtain the expression for the absorption cross section we extract the ingoing s-wave from the plane wave [50, 51]:

$$e^{i\omega z} \to \frac{\mathcal{K}}{(A_4 B)^{1/2} r^2} e^{-i\omega r} + (\text{higher multipole moments}), \tag{A22}$$

where the square root in the denominator is the normalization factor. In order to determine $\mathcal{K}$, one integrates both sides of Eq. (A22) over the 4-sphere with a deficit angle, and then, looking at the far region $\omega r \gg 1$, extracts only the ingoing modes. Thus, we arrive at

$$|\mathcal{K}|^2 = \frac{2^4(A_3)^2\Gamma^2(2)B}{4\omega^4 A_4} = \frac{6\pi^2 B}{\omega^4}, \tag{A23}$$

leading to the low energy absorption cross section

$$\begin{aligned} \sigma_0 &= |\mathcal{A}|^2|\mathcal{K}|^2 \\ &= \left[\frac{8\pi^2}{3} r_h^2(r_h^2+a^2)B\right] \frac{(1+a_*^2)}{(1+a_*^2/3)(2-\gamma)} + \cdots . \end{aligned} \tag{A24}$$

In the static limit we have $\sigma_0 =$ (horizon area), which reproduces the general result for the spherically symmetric case [50].

[1] N. Arkani-Hamed, S. Dimopoulos and G. R. Dvali, Phys. Lett. B **429**, 263 (1998) [arXiv:hep-ph/9803315]; N. Arkani-Hamed, S. Dimopoulos and G. R. Dvali, Phys. Rev. D **59**, 086004 (1999) [arXiv:hep-ph/9807344]; I. Antoniadis, N. Arkani-Hamed, S. Dimopoulos and G. R. Dvali, Phys. Lett. B **436**, 257 (1998) [arXiv:hep-ph/9804398].

[2] C. Kokorelis, Nucl. Phys. B **677**, 115 (2004) [arXiv:hep-th/0207234].

[3] L. Randall and R. Sundrum, Phys. Rev. Lett. **83**, 3370 (1999) [arXiv:hep-ph/9905221]; L. Randall and R. Sundrum, Phys. Rev. Lett. **83**, 4690 (1999) [arXiv:hep-th/9906064].

[4] S. B. Giddings and S. D. Thomas, Phys. Rev. D **65**, 056010 (2002) [arXiv:hep-ph/0106219]; S. Dimopoulos and G. L. Landsberg, Phys. Rev. Lett. **87**, 161602 (2001) [arXiv:hep-ph/0106295]; S. Hossenfelder, S. Hofmann, M. Bleicher and H. Stoecker, Phys. Rev. D **66**, 101502 (2002) [arXiv:hep-ph/0109085].

[5] D. M. Eardley and S. B. Giddings, Phys. Rev. D **66**, 044011 (2002) [arXiv:gr-qc/0201034]; H. Yoshino and Y. Nambu, Phys. Rev. D **66**, 065004 (2002) [arXiv:gr-qc/0204060]; H. Yoshino and Y. Nambu, Phys. Rev. D **67**, 024009 (2003) [arXiv:gr-qc/0209003]; E. Kohlprath and G. Veneziano, JHEP **0206**, 057 (2002) [arXiv:gr-qc/0203093]; E. Berti, M. Cavaglia and L. Gualtieri, Phys. Rev. D **69**, 124011 (2004) [arXiv:hep-th/0309203]; N. Kaloper and J. Terning, Gen. Rel. Grav. **39**, 1525 (2007) [arXiv:0705.0408 [hep-th]].

[6] S. W. Hawking, Commun. Math. Phys. **43**, 199 (1975) [Erratum-ibid. **46**, 206 (1976)].

[7] R. Emparan, G. T. Horowitz and R. C. Myers, Phys. Rev. Lett. **85**, 499 (2000) [arXiv:hep-th/0003118].

[8] P. Kanti and J. March-Russell, Phys. Rev. D **66**, 024023 (2002) [arXiv:hep-ph/0203223]; P. Kanti and J. March-Russell, Phys. Rev. D **67**, 104019 (2003) [arXiv:hep-ph/0212199].

[9] C. M. Harris and P. Kanti, JHEP **0310**, 014 (2003) [arXiv:hep-ph/0309054]; P. Kanti, J. Grain and A. Barrau, Phys. Rev. D **71**, 104002 (2005) [arXiv:hep-th/0501148]; S. Creek, O. Efthimiou, P. Kanti and K. Tamvakis, Phys. Lett. B **635**, 39 (2006) [arXiv:hep-th/0601126].

[10] C. M. Harris and P. Kanti, Phys. Lett. B **633**, 106 (2006) [arXiv:hep-th/0503010].

[11] G. Duffy, C. Harris, P. Kanti and E. Winstanley, JHEP **0509**, 049 (2005) [arXiv:hep-th/0507274].

[12] M. Casals, P. Kanti and E. Winstanley, JHEP **0602**, 051 (2006) [arXiv:hep-th/0511163]; M. Casals, S. R. Dolan, P. Kanti and E. Winstanley, JHEP **0703**, 019 (2007) [arXiv:hep-th/0608193].

[13] S. Creek, O. Efthimiou, P. Kanti and K. Tamvakis, Phys.

Rev. D **75**, 084043 (2007) [arXiv:hep-th/0701288]

[14] S. Creek, O. Efthimiou, P. Kanti and K. Tamvakis, arXiv:0707.1768 [hep-th].

[15] E. Berti, K. D. Kokkotas and E. Papantonopoulos, Phys. Rev. D **68**, 064020 (2003) [arXiv:gr-qc/0306106].

[16] D. Ida, Y. Uchida and Y. Morisawa, Phys. Rev. D **67**, 084019 (2003) [arXiv:gr-qc/0212035].

[17] Y. Morisawa and D. Ida, Phys. Rev. D **71**, 044022 (2005) [arXiv:gr-qc/0412070].

[18] V. Cardoso, G. Siopsis and S. Yoshida, Phys. Rev. D **71**, 024019 (2005) [arXiv:hep-th/0412138].

[19] V. Cardoso, M. Cavaglia and L. Gualtieri, Phys. Rev. Lett. **96**, 071301 (2006) [Erratum-ibid. **96**, 219902 (2006)] [arXiv:hep-th/0512002]; V. Cardoso, M. Cavaglia and L. Gualtieri, JHEP **0602**, 021 (2006) [arXiv:hep-th/0512116].

[20] P. Kanti and R. A. Konoplya, Phys. Rev. D **73**, 044002 (2006) [arXiv:hep-th/0512257]; P. Kanti, R. A. Konoplya and A. Zhidenko, Phys. Rev. D **74**, 064008 (2006) [arXiv:gr-qc/0607048].

[21] D. Ida, K. y. Oda and S. C. Park, Phys. Rev. D **67**, 064025 (2003) [Erratum-ibid. D **69**, 049901 (2004)] [arXiv:hep-th/0212108].

[22] D. Ida, K. y. Oda and S. C. Park, Phys. Rev. D **71**, 124039 (2005) [arXiv:hep-th/0503052].

[23] D. Ida, K. y. Oda and S. C. Park, Phys. Rev. D **73**, 124022 (2006) [arXiv:hep-th/0602188].

[24] V. P. Frolov and D. Stojkovic, Phys. Rev. D **67**, 084004 (2003) [arXiv:gr-qc/0211055].

[25] S. Creek, O. Efthimiou, P. Kanti and K. Tamvakis, arXiv:0709.0241 [hep-th].

[26] A. S. Cornell, W. Naylor and M. Sasaki, JHEP **0602**, 012 (2006) [arXiv:hep-th/0510009].

[27] H. T. Cho, A. S. Cornell, J. Doukas and W. Naylor, arXiv:0709.1661 [hep-th].

[28] P. Kanti, Int. J. Mod. Phys. A **19**, 4899 (2004) [arXiv:hep-ph/0402168].

[29] V. P. Frolov and D. Stojkovic, Phys. Rev. D **66**, 084002 (2002) [arXiv:hep-th/0206046]; V. P. Frolov, M. Snajdr and D. Stojkovic, Phys. Rev. D **68**, 044002 (2003) [arXiv:gr-qc/0304083]; V. P. Frolov, D. V. Fursaev and D. Stojkovic, JHEP **0406**, 057 (2004) [arXiv:gr-qc/0403002]; V. P. Frolov, D. V. Fursaev and D. Stojkovic, Class. Quant. Grav. **21**, 3483 (2004) [arXiv:gr-qc/0403054].

[30] D. M. Gingrich, JHEP **0711**, 064 (2007) [arXiv:0706.0623 [hep-ph]].

[31] D. C. Dai, G. Starkman, D. Stojkovic, C. Issever, E. Rizvi and J. Tseng, arXiv:0711.3012 [hep-ph].

[32] A. Flachi, O. Pujolas, M. Sasaki and T. Tanaka, Phys. Rev. D **74**, 045013 (2006) [arXiv:hep-th/0604139]; A. Flachi and T. Tanaka, Phys. Rev. Lett. **95**, 161302 (2005) [arXiv:hep-th/0506145]; A. Flachi and T. Tanaka, Phys. Rev. D **76**, 025007 (2007) [arXiv:hep-th/0703019].

[33] R. Emparan, G. T. Horowitz and R. C. Myers, JHEP **0001**, 007 (2000) [arXiv:hep-th/9911043].

[34] H. Kudoh, T. Tanaka and T. Nakamura, Phys. Rev. D **68**, 024035 (2003) [arXiv:gr-qc/0301089].

[35] S. Creek, R. Gregory, P. Kanti and B. Mistry, Class. Quant. Grav. **23**, 6633 (2006) [arXiv:hep-th/0606006].

[36] N. Tanahashi and T. Tanaka, arXiv:0712.3799 [gr-qc].

[37] F. R. Tangherlini, Nuovo Cim. **27**, 636 (1963); R. C. Myers and M. J. Perry, Annals Phys. **172**, 304 (1986).

[38] N. Kaloper and D. Kiley, JHEP **0603**, 077 (2006) [arXiv:hep-th/0601110].

[39] D. Kiley, arXiv:0708.1016 [hep-th].

[40] D. C. Dai, N. Kaloper, G. D. Starkman and D. Stojkovic, Phys. Rev. D **75**, 024043 (2007) [arXiv:hep-th/0611184].

[41] S. Chen, B. Wang and R. K. Su, Phys. Lett. B **647**, 282 (2007) [arXiv:hep-th/0701209].

[42] U. A. al-Binni and G. Siopsis, arXiv:0708.3363 [hep-th].

[43] H. T. Cho, A. S. Cornell, J. Doukas and W. Naylor, arXiv:0710.5267 [hep-th].

[44] C. M. Chambers, W. A. Hiscock and B. Taylor, Phys. Rev. Lett. **78**, 3249 (1997) [arXiv:gr-qc/9703018]; B. E. Taylor, C. M. Chambers and W. A. Hiscock, Phys. Rev. D **58**, 044012 (1998) [arXiv:gr-qc/9801044].

[45] H. Nomura, S. Yoshida, M. Tanabe and K. i. Maeda, Prog. Theor. Phys. **114**, 707 (2005) [arXiv:hep-th/0502179].

[46] E. W. Leaver, Proc. Roy. Soc. Lond. A **402** (1985) 285.

[47] E. Berti, V. Cardoso and M. Casals, Phys. Rev. D **73**, 024013 (2006) [Erratum-ibid. D **73**, 109902 (2006)] [arXiv:gr-qc/0511111].

[48] A. A. Starobinsky, JETP 37, 28 (1973); A. A. Starobinsky and S.M. Churilov, JETP 38, 1 (1973).

[49] M. Nozawa and K. i. Maeda, Phys. Rev. D **71**, 084028 (2005) [arXiv:hep-th/0502166].

[50] S. R. Das, G. W. Gibbons and S. D. Mathur, Phys. Rev. Lett. **78**, 417 (1997).

[51] S. R. Das and S. D. Mathur, Nucl. Phys. B **478**, 561 (1996) [arXiv:hep-th/9606185].